MADRID
inter.noise 2019
June 16 - 19
NOISE CONTROL FOR A BETTER ENVIRONMENT

Low frequency sound absorption and transmission loss of a tortuous waveguide-resonator system: Theory vs Experiment

Kalavsky, Eloise[1]
Acoustics Research Centre, University of Salford
The Crescent, M5 4LW, Salford, United Kingdom.

Venegas, Rodolfo[2]
Acoustics Research Centre, University of Salford
The Crescent, M5 4LW, Salford, United Kingdom.

ABSTRACT

This work investigates, theoretically and experimentally, the low-frequency acoustic behaviour of tortuous waveguides laterally loaded by acoustic resonators in reflection and transmission conditions. A homogenisation-based model has been used to design prototype metamaterials prior to experimental validation. The metamaterials exhibit a tunable sound absorption peak at a frequency significantly lower than the resonance frequency of the loading resonators. It is evidenced that an increase in the tortuosity of the waveguides can allow a reduction in thickness of the metamaterial, while maintaining or improving the key features of the low frequency absorptive spectrum. It is also shown that the addition of thin porous layers to the metamaterial can improve both the amplitude and bandwidth of the sound absorption peak while also controlling sound transmission via apparent visco-elastic effects.

Keywords: Sound attenuation, Metamaterials, Porous materials
I-INCE Classification of Subject Number: 30

1. INTRODUCTION

Using conventional porous or fibrous materials for low frequency sound absorption usually involves large or bulky absorbers [1], which is often undesired. This issue has motivated the design and development of compact materials for low frequency sound absorption. Previous work in this research area has shown that a periodic structure of a rigidly-backed slit waveguide plugged into a lattice of resonators [2] reduces the celerity of the sound wave propagating through the material and leads to a sub-wavelength peak

[1]e.kalavsky@edu.salford.ac.uk
[2]r.venegas@salford.ac.uk

in the sound absorption coefficient. Work in the design of microstructured materials [3, 4] showed that a waveguide combined with a lattice of cavities exhibits sub-wavelength sound absorptive peaks as a result of increasing the effective compressibility of the saturating fluid without altering its effective dynamic density. Also relevant to this paper is the work by Boutin and Bécot [5] on acoustics of rigidly-backed arrays of Helmholtz resonators that display sub-wavelength absorptive peaks well predicted by a model derived by homogenisation [6].

This paper investigates, theoretically and experimentally, the low-frequency acoustic behaviour of tortuous waveguides laterally loaded by acoustic resonators, referred to as metamaterials, in reflection and transmission conditions. Contrary to the cited works, the key role of the tortuosity of the waveguide is here evidenced by deriving a simple expression that predicts the frequency f_0 at which the first absorptive peak of the rigidly-backed metamaterial occurs. This expression reveals the influence of the geometrical parameters of the metamaterials on their sound absorptive behaviour. It is also shown that adding porous materials in the metamaterials can improve both the amplitude and bandwidth of sound absorption while also controlling sound transmission. Thus, adding porous materials in the metamaterial is proven to be an effective tuning strategy due to attenuation, primarily caused by visco-elastic effects.

To put forward the alluded concepts, a hybrid analytical-numerical approach is adopted to model the metamaterials with tortuous waveguides and their acoustic behaviour is confronted with that of metamaterials with straight waveguides, with the latter being modelled using a purely analytical approach. The acoustic properties predicted by the models for both type of metamaterials are compared with full visco-thermal finite element calculations and experimental data. This has shown validation of the developed models and we can conclude that these capture the physics correctly.

The rest of this paper is organised as follows. The theory behind sound absorption and sound transmission loss of the investigated metamaterials is outlined in Section 2. Analytical, numerical and experimental results are then discussed in Section 3. This is followed by concluding remarks in Section 4.

2. THEORY

2.2.1. Metamaterial modelling

The theory presented herein is applicable to metamaterials comprising of a waveguide laterally loaded by acoustic resonators. To simplify the presentation, we will consider a metamaterial with the specific geometries shown in Figure 1.

The metamaterial will be modelled as an equivalent fluid with effective properties. For simplicity, we will only consider a flow direction along the waveguide axis. In this case, the propagation of sound in the metamaterial is governed by the following Helmholtz equation for the acoustic pressure p.

$$\nabla^2 p + k_c^2 p = 0, \tag{1}$$

where the wave number k_c is given by

$$k_c(\omega) = \omega \sqrt{\frac{\eta \mathsf{C}}{j\omega\mathcal{K}}}. \tag{2}$$

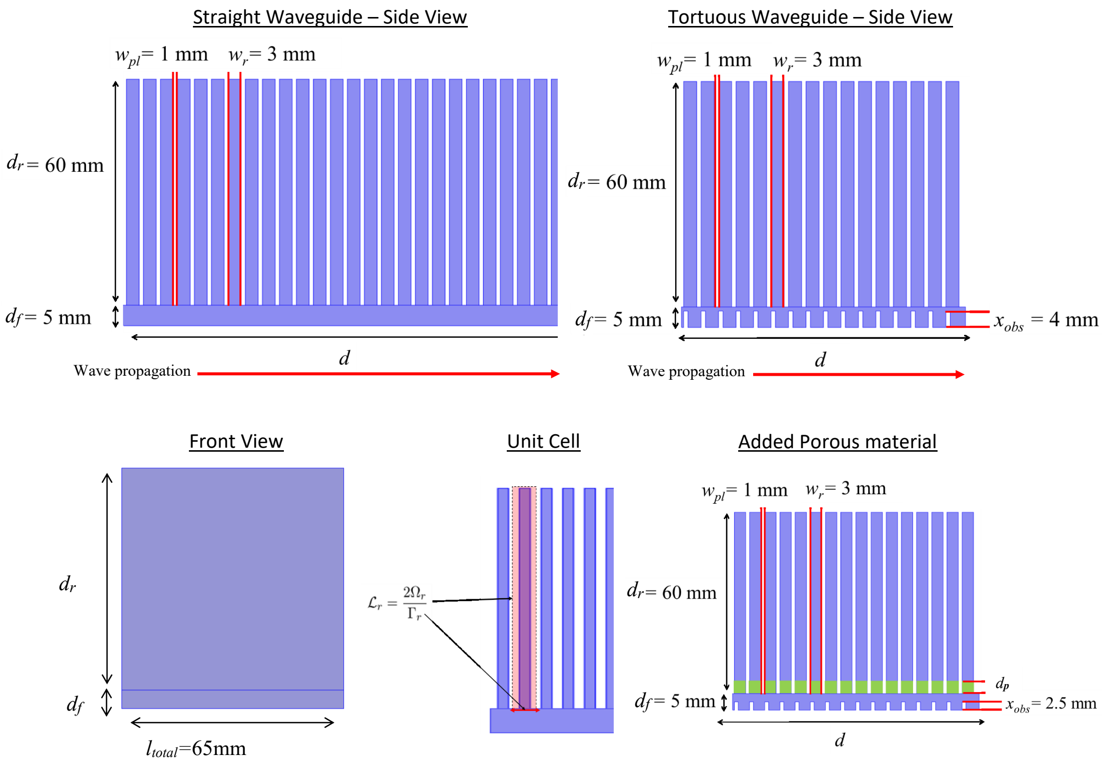

Figure 1: Diagram of the straight waveguide (top left) and tortuous waveguide (top right) laterally loaded with quarter wavelength resonators, plus the tortuous waveguide with added porous material (bottom right). The red arrows indicate the direction of sound propagation through the metamaterial.

Here, ω is the angular frequency, η is the dynamic viscosity, $\mathcal{K} = \varphi_f \mathcal{K}_f$ is the dynamic viscous permeability[7, 5] of the metamaterial, φ_f is the volume fraction occupied by the tortuous waveguide and $\mathcal{K}_f$ is its dynamic viscous permeability. The effective compressibility of the metamaterial C is estimated as [7, 5]

$$\mathsf{C}(\omega) = \varphi_f \mathsf{C}_f + \varphi_r \phi_{rs} \frac{2}{\mathcal{L}_r} \frac{\mathcal{Y}_r}{j\omega}, \tag{3}$$

where φ_r is the volume fraction occupied by resonators, the surface porosity, defined as the fraction of area occupied by the fluid on the interface between the waveguide and the surface of the resonator unit cell facing it, is denoted as ϕ_{rs}; the characteristic length $\mathcal{L}_r$ is defined as twice the volume occupied by the resonators Ω_r divided by the area of the surface of the resonator unit cell facing the tortuous waveguide (see Figure 1), i.e. $\mathcal{L}_r = 2\Omega_r/\Gamma_r$; and $\mathcal{Y}_r$ is the effective admittance of the loading resonators, which reads as [7, 5]

$$\mathcal{Y}_{eff}(\omega) = Z_{wr}^{-1} \quad \text{with} \quad Z_{wr}(\omega) = -jZ_r \cot(k_r d_r), \tag{4}$$

where Z_r and k_r are the characteristic impedance and wave number of the slit-shaped quarter-wavelength resonators.

Using the following expression for the characteristic impedance Z_c of the metamaterial

$$Z_c(\omega) = \sqrt{\frac{\eta}{j\omega \mathcal{K} \mathsf{C}}}, \tag{5}$$

one can calculate the normalised surface impedance z_w and sound absorption coefficient $\mathcal{A}$ of a rigidly-backed layer of thickness d as

$$z_w(\omega) = -j\frac{Z_c}{Z_0}\cot(k_c d) \quad \text{and} \quad \mathcal{A}(\omega) = \frac{4\mathrm{Re}(z_w)}{(1+\mathrm{Re}(z_w))^2 + (\mathrm{Im}(z_w))^2} \tag{6}$$

where $Z_0 = \rho_0 c_0$ is the characteristic impedance of the fluid adjacent to the metamaterial layer and ρ_0 and c_0 are its density and speed of sound, respectively.

The sound transmission loss TL of a finite metamaterial layer with thickness d can be calculated as [1]

$$\mathrm{TL}(\omega) = 20\log\left(\left|\cos(k_c d) + j\sin(k_c d)\frac{1}{2}\left(\frac{Z_c}{Z_0} + \frac{Z_0}{Z_c}\right)\right|\right) \tag{7}$$

Introducing a porous layer with thickness d_p in the metamaterial, as depicted in Figure 1, leads to replace the effective admittance Equation 4 by

$$\mathcal{Y}_{eff} = \frac{Z_{wp} + Z_{wr}}{Z_{wp}Z_{wr} + Z_p^2} = Z_{eff}^{-1} \quad \text{with} \quad Z_{wp} = -jZ_p\cot(k_p d_p), \tag{8}$$

where k_p and Z_p are the wave number and characteristic impedance of the porous layer. Note that the thickness d_r in Equation 4 is that of the slit-shaped resonator without including that of the porous layer.

2.2.2. Analysis of the metamaterials acoustical properties

Let us consider the case where sound propagation in the tortuous waveguide is adiabatic. This means that the effective compressibility of the tortuous waveguide can be approximated by [8] $\mathsf{C}_f \approx \phi_f/\gamma P_0$ and the dynamic viscous permeability of the metamaterial is estimated as [1] $\mathcal{K} \approx \varphi_f\phi_f\eta/j\omega\rho_0\alpha_{\infty f}$, where ϕ_f and $\alpha_{\infty f}$ are the internal porosity and the tortuosity of the tortuous waveguide, respectively. Furthermore, assuming adiabatic sound propagation in the slit-shaped resonators and $|k_r d_r| << 1$ leads to approximating the effective admittance by $\mathcal{Y}_{eff} \approx j\omega d_r/\gamma P_0$. Hence the effective compressibility of the metamaterial takes the asymptotic value $\mathsf{C} \approx \Phi/\gamma P_0$, where $\Phi = \varphi_f\phi_f + \varphi_r\phi_{rs}$ is the total porosity of the metamaterial.

Inserting the approximated values of the effective properties into Equation 6 yields a purely imaginary normalised surface impedance that vanishes when the argument of the cotangent is equal to $\pi/2$. This leads to estimate the following resonance frequency f_0 at which a first peak in the sound absorption coefficient of a rigidly-backed metamaterial layer appears:

$$f_0 = \frac{c_0}{4d}\frac{1}{\sqrt{\alpha_{\infty f}}}\sqrt{\frac{\varphi_f\phi_f}{\Phi}} \tag{9}$$

This equation is a key result of this work and reveals that by increasing the tortuosity of the waveguide, f_0 can be reduced. At the same time, it is clear that increasing the tortuosity permits reducing the thickness of the metamaterial, while maintaining f_0. It is also worth highlighting that f_0 is smaller than both the resonance frequency of the loading resonators $f_r = c_0/4d_r$, and the usual quarter-wavelength resonance frequency associated with the metamaterial thickness $f_q = c_0/4d$.

Introducing a thin porous layer in the metamaterial, as depicted in Figure 2, adds losses in the system. Assuming that sound propagation in the thin porous layer is isothermal and considering the same approximations as in the previous paragraphs leads to estimating the effective impedance in Equation 8 by $Z_{eff} \approx (j\omega d_r(1+\chi)/\gamma P_0)^{-1} + \tilde{\sigma}/(1+\chi)$, where $\chi = \gamma\phi_p d_p/d_r$ and $\tilde{\sigma}$ is the flow resistance of the porous material (i.e. the static flow resistivity σ_{0p} times the layer thickness d_p). Defining $d_q = d_p + d_r$ and recalling that $\mathcal{L}_r = 2d_q$, $\varphi_p = d_p/d_q$, and $1-\varphi_p = d_r/d_q$, the effective compressibility of the metamaterial can be approximated by

$$\mathsf{C}(\omega) \approx \frac{\varphi_f}{K_f} + \frac{\varphi_r\phi_{rs}}{K_{pr}\left(1+\frac{j\omega}{\omega_{pr}}\right)} \quad \text{with} \quad K_f = \frac{\gamma P_0}{\phi_f}, \tag{10}$$

$$K_{pr} = \frac{\gamma P_0}{\gamma\varphi_p\phi_p + (1-\varphi_p)\phi_r} \quad \text{and} \quad \omega_{pr} = \frac{\gamma P_0}{\sigma_{0p}}\frac{1}{\varphi_p(1-\varphi_p)d_q^2},$$

where K_{pr} is the apparent bulk modulus of the porous layer-resonator system and ω_{pr} is a visco-elastic characteristic frequency.

Following the procedure outlined above leads to a complex surface impedance of the metamaterial and further analysis reveals that the absorptive peak centred around f_0 becomes wider. This will be exemplified in the next section.

Supposing that $|k_c d| << 1$, the sound transmission loss can be approximated by [9]

$$\text{TL}(\omega) \approx 20\log\left(\left|1 + \left(\frac{\eta}{\mathcal{K}}\frac{1}{Z_0} + j\omega\mathsf{C}Z_0\right)\frac{d}{2}\right|\right) \tag{11}$$

This expression shows that the sound transmission behaviour is largely controlled by the effective compressibility. This is because the dynamic viscous permeability of the metamaterial with and without a thin porous layer is approximately the same, while the effective compressibility is significantly modified. In particular, introducing a thin porous layer in the metamaterial leads to a larger TL caused by visco-elastic effects (see Equation 10), as will be exemplified below.

3. RESULTS

This section presents the hybrid analytical-numerical predictions for the metamaterial configurations shown in Figure 1. These predictions have been validated numerically using full visco-thermal finite element calculations. Both have been compared to experimental results obtained from a prototype measured in an impedance tube by following the procedure described in [10].

3.3.1. Sound absorption coefficient

The sound absorption coefficient $\mathcal{A}$ is calculated using Equation 6. This depends on the effective properties of the metamaterial given by Equation 5 and Equation 2. These require knowing i) the dynamic viscous permeability and effective compressibility of the tortuous waveguide, which are calculated using semi-phenomenological models [11, 8] with numerically calculated input parameters (see e.g. [9] for the calculation procedure), and ii) the effective parameters of the slit-shaped resonator, which are calculated analytically (see e.g. equations 71 and 72 in [12]).

Figure 2 shows the sound absorption coefficient $\mathcal{A}$ of a rigidly-backed layer of the metamaterial with a tortuous waveguide, where the first peak occurs at $f_0 = 250.2Hz$. This compared with that of a metamaterial with straight waveguide having the same thickness,

Table 1: Nominal values of the geometrical parameters of the metamaterials with a straight waveguide (SW) and a tortuous waveguide (TW).

	d_f[mm]	d_r[mm]	w_{pl}[mm]	w_r[mm]	x_{obs}[mm]	d[mm]	ϕ_f	$\alpha_{\infty f}$
SW	5	60	1	3	0	120	1	1
TW	5	60	1	3	4	64	0.8	2.82

where in this case $f_0 = 228.9Hz$. The geometrical parameters of the metamaterials are shown in Table 1.

It is clear from Figure 2 that a good agreement between the models predictions and full visco-thermal finite element calculations is achieved. Moreover, the figure evidences that increasing the tortuosity of the waveguide allows for a reduction in the metamaterial thickness and an improvement of the amplitude of the peak at f_0.

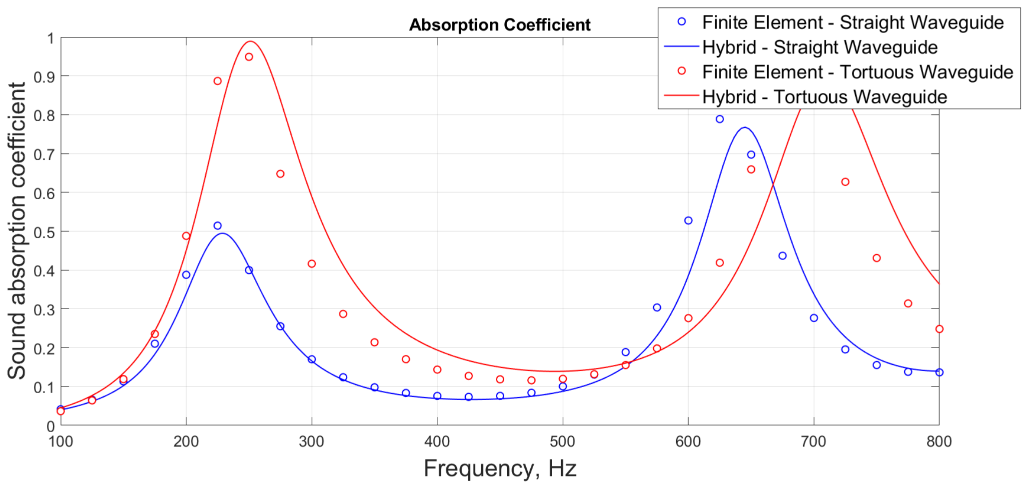

Figure 2: Sound absorption coefficient of the tortuous waveguide and straight waveguide: Predictions (lines) vs Finite element calculations (circles).

Metamaterials having the geometries shown in Figure 1 were hand-made using alternating 1mm (w_{pl}) and 3mm (w_r) aluminium plates to create resonator walls and cavities respectively. These were then fixed to a base plate with a hollowed central section creating the waveguide. The whole metamaterial was fixed to an adapting plate to allow for securing to the impedance tube with only the waveguide "visible" to the incident sound. Figure 3 shows the experimental validation of the theory. From this figure, it can be seem that the experimental data validates the theory. For example, the identified frequency f_0 is predicted with an error of less than 1.9% and 6.5 % for the metamaterial with tortuous and straight waveguide, respectively. In this case, f_0 for the tortuous waveguide was measured to be $254.8Hz$ and for the straight waveguide was $214.4Hz$. There is an evident discrepancy between the hybrid and finite element results and the experimental results for the amplitude at f_0 for both of the metamaterials. This may due to the uncertainty involved in the hand-made building of the prototype metamaterials and possible small gaps in between the plates forming the loading resonators that increases the damping in the system. Similar trends have been found in a parametric analysis, not presented here for the sake of brevity, that shows that small variations in obstacle size can have a large effect on the amplitude of the absorptive peak. It is now known that the experimental results for the tortuous waveguide are more representative of a metamaterial with obstacles smaller than the nominal size by approximately less than 1 mm. This finding reveals the very high sensitivity of the acoustic response of the metamaterials and highlights the need for precise metamaterial manufacturing.

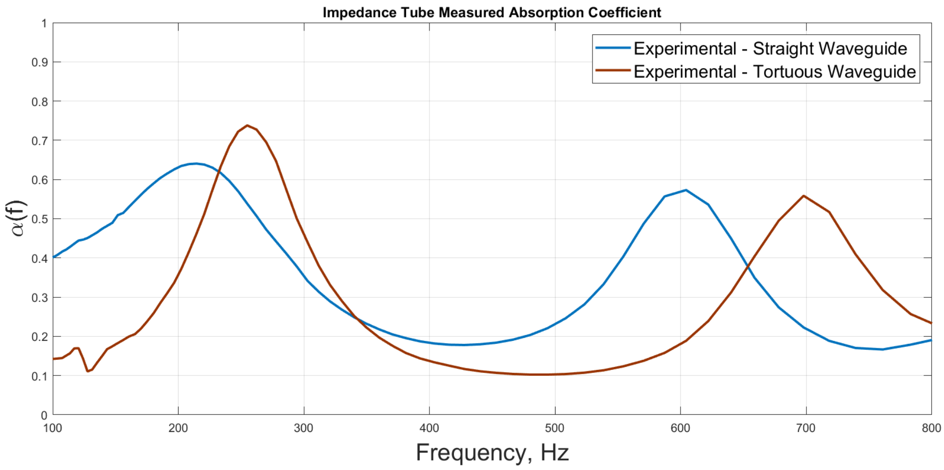

Figure 3: Measured sound absorption coefficient of the straight and tortuous waveguide prototypes

When a layer of thin porous material is added to the entrance of each resonator, the bandwidth of the absorptive peak is increased, as evidenced in Figure 4. To better illustrate this effect, the obstacle height in the tortuous waveguide is decreased to 2.5 mm and total metamaterial thickness is 64 mm while the rest of the parameters remain as in Table 1, with exceptions being $\phi_f = 0.88$ and $\alpha_{\infty f} = 1.49$.

From this, it is evident as the thickness and flow resistance of the porous material is increased the effective impedance becomes much larger and thus a damping effect occurs. This gives a smaller amplitude and larger bandwidth peak at f_0 and evidences that the addition of porous media can allow tuning of the metamaterial.

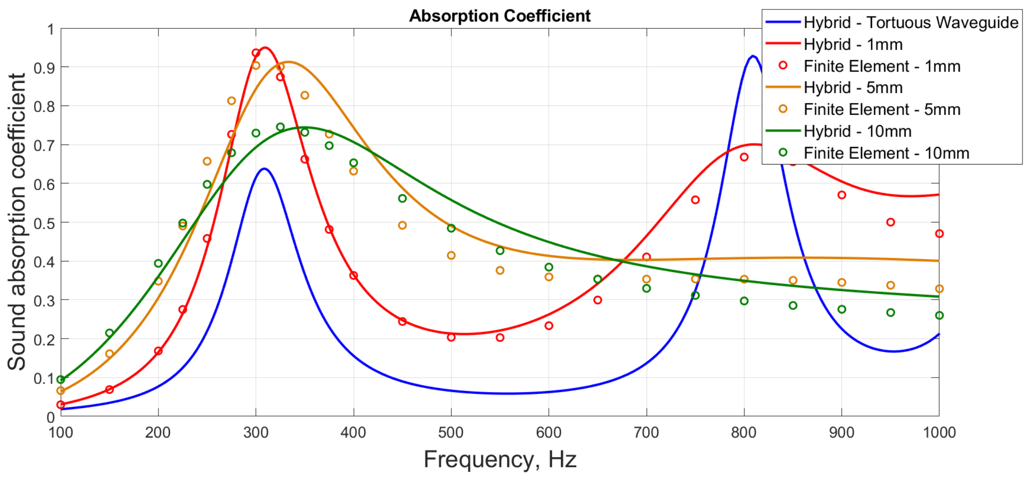

Figure 4: Sound absorption coefficient of a metamaterial with varying thickness of porous material (d_p = 1mm, 5mm and 10mm)

3.3.2. Sound transmission loss

Having validated the hybrid analytical-numerical model by comparing its prediction with both full numerical simulations and experimental data, the hybrid model is now used to evaluate the sound transmission behaviour of the metamaterial.

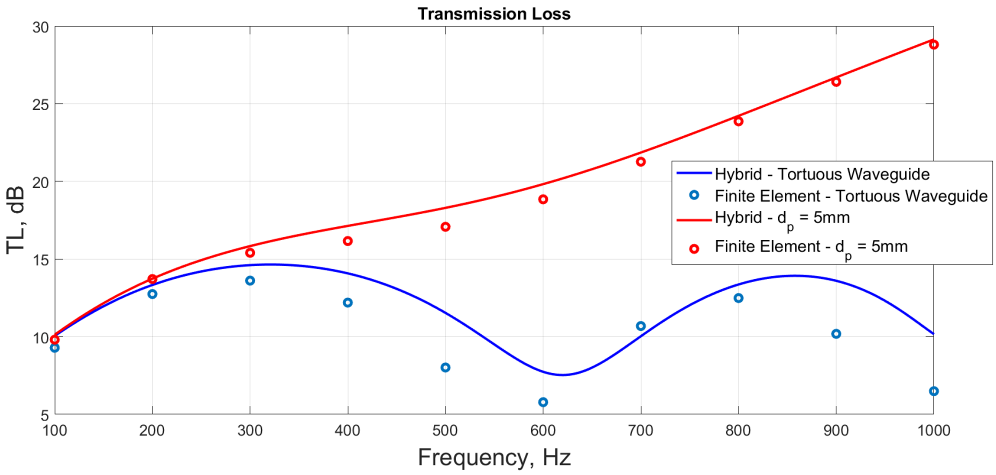

Figure 5: TL *of a tortuous waveguide without a porous layer versus tortuous waveguide with porous layer of 5mm thickness: Predictions (lines) versus Finite element calculations (circles)*

Figure 5 shows the sound transmission loss of tortuous waveguide of the same geometry as used in Figure 4 compared to the same waveguide with 5 mm of porous material introduced to the entrance of the quarter-wavelength resonators. It is evident from Figure 5 that an agreement between the hybrid-analytical results and numerical model exists. The results also show that for the tortuous waveguide without the porous material a small peak in transmission loss exists before a decrease and then another small peak, following the pattern seen in a simple expansion chamber [13]. However, the addition of 5 mm of porous material nullifies the existence of this decrease and allows the metamaterial to show continuous improvement in sound transmission loss as frequency increases, which is a result similar to those found in dissipative silencers [14]. Ongoing experimental work on sound transmission loss of the metamaterials will be presented in the conference.

4. CONCLUSIONS

A homogenisation-based model has been taken to firstly theoretically investigate a rigidly-backed waveguide laterally loaded by quarter-wavelength resonators in reflection and transmission conditions. Using this model, a formula has been derived for the frequency f_0 at which the first absorption peak occurs. This formula reveals the key role the waveguide tortuosity plays for sound absorption purposes and how it allows for a more compact metamaterial while maintaining the same absorption characteristics which has been evidenced by an agreement between hybrid analytical-numerical models and visco-thermal finite element calculations. Further experimental validation in reflection condition has taken place which concludes that the physics is well captured and the theory proven. When porous media is introduced to this metamaterial it has been presented that this effectively tunes the metamaterial by apparent visco-elastic effects, however this can produce over-damping of the absorptive peaks.

In transmission condition, the addition of this porous media has allowed for a continuous increase in sound transmission loss whereas without the porous media there are small increases and decreases. This metamaterial with added porous media allows for an effective transmission loss without blockage of an air flow path, presenting an interesting approach to increasing sound transmission loss as evidenced both analytically and numerically. Further work will see experimental validation of the addition of porous media and sound transmission loss predictions.

5. ACKNOWLEDGEMENTS

We gratefully acknowledge Mike Clegg for his skill and contributions to the building of the metamaterial prototype.

6. REFERENCES

[1] J. F. Allard and N. Atalla. *Propagation of Sound in Porous Media: Modeling Sound Absorbing Materials*. John Wiley & Sons, 2009.

[2] J. P. Groby, A. Lardeau, W. Huang, and Y. Auregan. The use of slow sound to design simple sound absorbing materials. *J. Appl. Phys.*, 117:124903, 2015.

[3] P. Leclaire, O. Umnova, T. Dupont, and R. Panneton. Acoustical properties of air-saturated porous material with periodically distributed dead-end pores. *J. Acoust. Soc. Am.*, 137(4):1772–1782, 2015.

[4] T. Dupont, P. Leclaire, R. Panneton, and O. Umnova. A microstructure material design for low frequency sound absorption. *Appl. Acous.*, 136:86–93, 2018.

[5] C. Boutin and F. X. Becot. Theory and experiments on poro-acoustics with inner resonators. *Wave Motion*, 54:76–99, 2015.

[6] J. L. Auriault, C. Boutin, and C. Geindreau. *Homogenization of Coupled Phenomena in Heterogeneous Media*. ISTE Ltd and John Wiley & Sons, 2009.

[7] E. Kalavsky and R. Venegas. Low-frequency sound absorption of rigidly-backed waveguides laterally loaded by acoustic resonators. In *Symposium on Acoustic Metamaterials*, Xativa, Spain, 7th–9th November 2018.

[8] D. Lafarge, P. Lemarinier, J. F. Allard, and V. Tarnow. Dynamic compressibility of air in porous structures at audible frequencies. *J. Acoust. Soc. Am.*, 102(4):1995–2006, 1997.

[9] R. Venegas. *Microstructure influence on acoustical properties of multiscale porous materials*. PhD thesis, University of Salford, Salford, United Kingdom, 2011.

[10] Acoustics–Determination of sound absorption coefficient and impedance in impedance tubes–Part 2: Transfer-function method. Standard, International Organization for Standardization, Geneva, CH, 2001.

[11] D. L. Johnson, J. Koplik, and R. Dashen. Theory of dynamic permeability and tortuosity in fluid-saturated porous media. *J. Fluid Mech.*, 176:379–402, 1987.

[12] R. Venegas and C. Boutin. Acoustics of sorptive porous materials. *Wave Motion*, 68:162–181, 2017.

[13] M. L. Munjal. *Acoustics of Ducts and Mufflers*. Wiley, 2 edition, 2014.

[14] R. Venegas, J.P. Arenas, and C. Boutin. Analytical modeling of dissipative silencers. *J. Acoust. Soc. Am.*, 144(5):2998–3009, 2018.